

# Practical Marketplace Optimization at Uber Using Causally-Informed Machine Learning

Bobby Chen\*<sup>†</sup>  
 Siyu Chen\*  
 Jason Dowlatabadi\*  
 Yu Xuan Hong\*  
 Vinayak Iyer\*  
 Uday Mantripragada\*

Rishabh Narang\*  
 Apoorv Pandey\*  
 Zijun Qin\*  
 Abrar Sheikh\*  
 Hongtao Sun\*<sup>†</sup>  
 Jiaqi Sun\*  
 Uber Technologies, Inc  
 San Francisco, CA, USA  
 mhwalker,zijunq@uber.com

Matthew Walker\*  
 Kaichen Wei\*  
 Chen Xu\*  
 Jingnan Yang\*  
 Allen T. Zhang\*  
 Guoqing Zhang\*

## ABSTRACT

Budget allocation of marketplace levers, such as incentives for drivers to complete certain trips or promotions for riders to take more trips have long been both a technical and business challenge at Uber. It is crucial to understand the impact of lever budget changes on the market and to estimate their cost efficiency given the need to achieve predefined budgets, where the eventual goal is to find the optimal allocations under those constraints that maximize some objective of value to the business. In this paper, we introduce an end-to-end machine learning and optimization procedure to automate budget decision-making for cities where Uber operates. This procedure relies on a suite of applications, including feature store, model training and serving, optimizers and backtesting to measure the prediction and causal accuracy. We propose a state-of-the-art deep learning (DL) estimator based on S-Learner that leverages massive amount of user experimental and temporal-spatial observational data. We also built a novel tensor B-Spline regression model to enforce efficiency shape control while retaining the sophistication of the DL models' response surface, and solved the high-dimensional optimization problem with Alternating Direction Method of Multipliers (ADMM) and primal-dual interior point convex optimization. This procedure has demonstrated substantial improvement in Uber's ability to allocate resources efficiently.

## CCS CONCEPTS

• **Computing methodologies** → **Machine learning algorithms**;  
 • **General and reference** → *Measurement*; • **Mathematics of computing** → **Mathematical optimization**.

\*Authors listed alphabetically.

<sup>†</sup>Formerly at Uber Technologies, Inc.

Permission to make digital or hard copies of all or part of this work for personal or classroom use is granted without fee provided that copies are not made or distributed for profit or commercial advantage and that copies bear this notice and the full citation on the first page. Copyrights for components of this work owned by others than the author(s) must be honored. Abstracting with credit is permitted. To copy otherwise, or republish, to post on servers or to redistribute to lists, requires prior specific permission and/or a fee. Request permissions from [permissions@acm.org](mailto:permissions@acm.org).  
*KDD 2024 Workshop, August 25–26, 2024, Barcelona, Spain*

© 2024 Copyright held by the owner/author(s). Publication rights licensed to ACM.  
 ACM ISBN 978-1-4503-XXXX-X/18/06...\$15.00  
<https://doi.org/XXXXXXXX.XXXXXXX>

## KEYWORDS

Causal machine learning, deep neural network, convex optimization, shape-constrained, measurement

### ACM Reference Format:

Bobby Chen, Siyu Chen[1], Jason Dowlatabadi[1], Yu Xuan Hong[1], Vinayak Iyer[1], Uday Mantripragada[1], Rishabh Narang[1], Apoorv Pandey[1], Zijun Qin[1], Abrar Sheikh[1], Hongtao Sun[1][2], Jiaqi Sun[1], Matthew Walker[1], Kaichen Wei[1], Chen Xu[1], Jingnan Yang[1], Allen T. Zhang[1], and Guoqing Zhang[1]. 2024. Practical Marketplace Optimization at Uber Using Causally-Informed Machine Learning. In *Proceedings of 2nd Workshop on Causal Inference and Machine Learning in Practice (KDD 2024 Workshop)*. ACM, New York, NY, USA, 10 pages. <https://doi.org/XXXXXXXX.XXXXXXX>

## 1 INTRODUCTION

Each year, Uber manages a multi-billion dollar marketplace. In the third quarter of 2023 alone [1], Uber's mobility business recorded \$17.9 billion in Gross Bookings (GBs). To attract riders and drivers to use the products and to influence the behavior of the marketplace, Uber invests in various marketplace levers, allocating budgets across different regions and lever types to optimize business objectives. Historically, budget allocation was done manually, with teams reviewing data and adjusting numbers in spreadsheets based on personal experience and past allocations. This method did not effectively utilize historical data on rider and driver behavior under different conditions, lacked a clear objective, and was labor-intensive, making it difficult to measure its effectiveness quantitatively. We present an automated system that leverages causal deep learning models to predict how each marketplace lever affects driver and rider behavior and a set of optimization algorithms to decide optimal budget allocation across levers and regions. The causal deep learning model leverages historical data to predict supply, demand, and a custom marketplace objective in the upcoming week for each region and a given set of incentives. The system then uses a smoothing model to generate high level functions between incentive budgets and the outcome for the optimization stage. Finally, the system finds the optimal budget allocation for each region and incentive lever subject to business operations constraints, using an optimization system to solve a non-convex problem. In addition, we also devised a framework and system to measure the business impact of the budget allocation when compared to a baseline allocation. This system is deployed in production on a weekly basis

to allocate incentive budgets, and is proven to generate significant impact to Uber’s business. This work contains the following contributions:

- Introducing a novel S-Learner architecture that combines temporal-spatial observational data with finer-granularity experimental data in its learning objective.
- Developing a student model technique using b-splines that enforces efficiency, business intuition, and teacher model response shape control while marginalizing non-control features.
- Creating a fully distributed optimizer using ADMM and primal-dual interior point convex optimization, implemented on Ray to handle complex, nonlinear, non-convex problems.
- Proposing a new method for evaluating counterfactual outputs without a clean experimental environment for standard approaches like Randomized Control Trials (RCTs) or switchbacks.

## 2 BACKGROUND AND RELATED WORK

Uber, being a publicly traded company, gives guidance to the public about expectations for performance on certain business metrics for each quarter. Two important metrics are Gross Bookings (GB), which is a measure of how much business was conducted on the Uber platform, and Net Income (NI), which is the generally accepted accounting practice definition of profit [1]. The internal teams at Uber must make prediction on how different products can affect market and therefore affect the key financial metrics. This financial task can be formulated as follows:

$$\begin{aligned}
 & \text{maximize} && \sum_{w \in \text{weeks}, c \in \text{cities}} && obj_{w,c}(\mathbf{b}_{w,c}) \\
 & \text{subject to} && \sum_{w \in \text{weeks}, c \in \text{cities}, l \in \text{levers}} && b_{w,c,l} = B \\
 & && && b_{w,c,l} \geq h_{w,c,l} \\
 & && && b_{w,c,l} \leq g_{w,c,l}
 \end{aligned} \tag{1}$$

where weeks are calendar weeks, cities are approximately independent geographical entities, and levers are different marketplace programs that Uber can allocate money to in order to affect marketplace outcomes. The function  $obj$  is some objective of importance to the business. The variables  $b_{w,c,l}$  represent budgets for specific weeks, cities, and levers, which can be positive or negative; we use the convention that positive budgets correspond to Uber spending. The variable  $B$  is a total budget constraint on the system. The variables  $h_{w,c,l}$  and  $g_{w,c,l}$  represent floors and ceilings, respectively, on how much money can be spent in a lever in a specific city-week, which can again be positive or negative.

The objective of Equation 1 is to maximize business throughput subject to a fixed budget constraint. The challenge is that the effects of budgeting a certain lever may not be linear and there may be substantial interaction effects between levers. In the following discussion, we confine ourselves to discussing only Uber’s Rides business and further confine the problem to a single week and the budgets are full-week treatments.

### 2.1 Causal Marketplace Forecasting

A critical component of solving this problem is how well we can predict the impact of changing the budgets under our control on

$obj$ . Imagine a world that is described by an oracle:

$$obj(\mathbf{b}, \mathbf{X}) \tag{2}$$

where  $\mathbf{b}$  and  $\mathbf{X}$  are the feature vectors for anything under our control and not under our control.

Our task is to produce an estimator of that oracle for a future week:

$$\widehat{obj}(\widehat{\mathbf{b}}, \widehat{\mathbf{X}}), \tag{3}$$

where  $\widehat{\mathbf{b}}$  is what we believe the feature vector under our control will be valued and  $\widehat{\mathbf{X}}$  is what we predict any feature of interest will be valued. Importantly,  $dim(\mathbf{b}) \stackrel{?}{=} dim(\widehat{\mathbf{b}})$  and  $dim(\mathbf{X}) \stackrel{?}{=} dim(\widehat{\mathbf{X}})$ , which is to say, neither control variables nor other confounding features can be guaranteed to be observed. The control variables have continuous values, in this case budgets.

Let us consider how data can be collected in this context. We are concerned with *marketplace* outcomes, which are outcomes aggregated over some finer granularity. In our case, we are looking at outcomes aggregated per city per week. The finer granularity, in the case of Uber, could be riders, drivers, trips, etc. In a marketplace, it is generally assumed that there can be interference effects between treatment groups during experiments[31]. Therefore, experimental results obtained by conducting a randomized controlled trial on a higher granularity treatment entity may not extrapolate to applying a treatment to the entire population of treated entities.

Since the standard assumptions of collecting unconfounded, independent, and identically distributed data do not apply, we can not rely on standard techniques or bounds to guarantee performance of any estimator. Instead, we must develop empirical techniques against which to test any estimator using both predictive accuracy, referring to how well absolute outcomes of the estimator agree with test data, as well as causal accuracy, referring to how well derivatives of the estimator agree with test data.

### 2.2 Related Work

**Time series forecasting** continues to be an area of significant interest in the literature. Autoregressive statistical approaches related to ARIMA [11] remain performant in certain domains, including stock prediction [5] and pandemic spread [8] prediction. In light of the success of transformers [46] in the natural-language processing space, many proposals have been made to apply transformers to time series prediction problems in order to model both multi-variate dependencies and overall complexity in the time series [34, 35, 51–53]. Recent results showing the effectiveness of simple linear models on standard datasets [49] has led to additional recent work on MLP-only approaches [17]. In contrast to the literature mentioned above, which focuses primarily on high predictive accuracy, as measured generally by mean-squared error (MSE) and mean absolute error (MAE), we are concerned also with causal accuracy of the model. Furthermore, identification of a generally superior model architecture has so far defied researchers in the time series forecasting space, so performant models in new domains remain of interest.

**Causal ML** approaches have explored how to infer heterogeneous treatment effects using multiple different strategies[7, 21, 25, 30, 32, 40, 43] and showing that, under certain conditions, certain error terms can be substantially reduced[18, 33, 39]. This body of work nearly entirely relies on two assumptions that we cannot rely

on in practical marketplace applications. Relying on the notation that  $X_i$  are per-unit features,  $Y_i \in \mathbb{R}$  is the observed treatment effect and  $W_i \in \{0, 1\}$  is the binary treatment assignment, the first assumption is that the treatment assignment  $W_i$  is unconfounded, i.e.  $\{Y_i(0), Y_i(1)\} \perp W_i | X_i$  [39]. This is nearly always false in any available observational marketplace data. To give an obvious example: larger cities have larger budgets. The second assumption is that any data of interest is independent and identically distributed. Neither of these conditions hold under realistic marketplace conditions. An example of the first is that the level of treatment in one week may impact how users return in the following week, resulting in different returns. An example of the second is that there could be a major sporting event one week that results in very different user behavior compared to any other week. While some of the techniques are informative, the theoretical findings have no applicability to the practical case.

### 3 METHODOLOGY

In this section, we will focus on details of key components of the budget allocation system: the user causal effect estimator, smoothing layer with B-Spline functions, optimizer and the business value evaluation framework. A diagrammatic view of the entire system can be found in Appendix A.

#### 3.1 User Causal Effect Estimator

To better leverage A/B experiments data which contains the information of user behaviors between treatment and control groups, We adopted the S-metalearner [33] framework with a ResNet[27] model to estimate individual treatment effects (ITE).

We have explored other metalearners such as the stacked R-metalearner, and the decision towards S-metalearner took various considerations into account including feasibility of available computing resources, the implementation and maintenance efforts required from a practical standpoint, and experiment results in Appendix B show S-metalearner provided better incremental efficiency with diminishing returns, aligning well with business intuition.

As illustrated in Fig. 1, the model consists of two stages:

##### Embedding stage

- *Sparse embeddings.* Our input features consist of some categorical sparse features. Since DNN’s are usually good at handling dense numerical features, we map the sparse features into trainable dense vectors using embeddings.
- *Dense feature extractor.* We also extract an embedding representation for dense numerical features in order to better capture higher order interactions between the dense features. The dense feature embeddings are generated through multilayer perceptrons[26] (MLP).

**Residual network stage.** Sparse and dense feature embeddings are concatenated and fed into a series of ResNet blocks and eventually generate predictions. ResNet blocks are chosen instead of MLP in order to better handle vanishing gradients and reduce the risk of overfitting when feature sizes are large.

During analysis of deployed budget recommendations, we also diagnosed and resolved an endogeneity [29] issue that is naturally introduced from clustering data across cities and weeks during model training. It led to possible cross week extrapolations as the

training data from different weeks could be endogenous and more severely, the treatment-control effects are masked out by cross-week data. This issue was resolved by adding additional positional encoding for the week in the training and serving data.

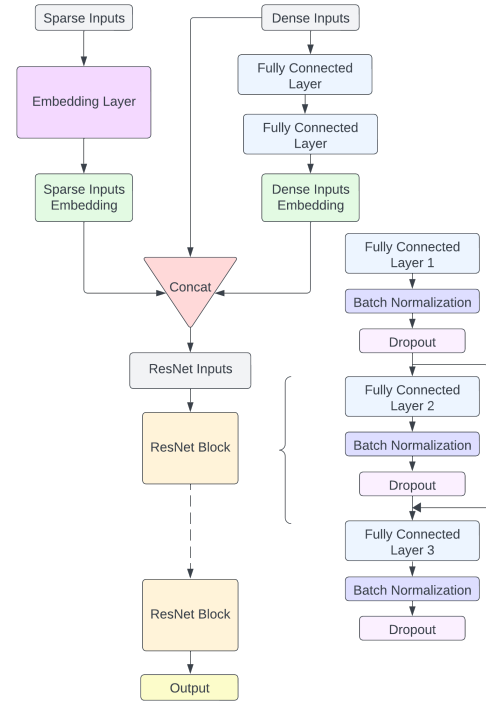


Figure 1: Driver model base learner architecture

#### 3.2 Smoothing Layer

The DL model in Section 3.1 produces a mapping from budgets to marketplace outcomes, which can be fed into an optimizer. However, most optimization routines require numerous passes over the surface, necessitating many evaluations of the DL model, which is computationally costly, potentially prohibitively so. Additionally, the mapping produced by DL models does not necessarily satisfy business intuition (e.g., non-negativity, monotonicity, convexity). Enforcing such business intuition using flexible functional forms is generally intractable. For instance, verifying polynomial non-negativity [10] and convexity [2] is NP-hard.

Our goal is to generate a differential surface for derivative-based optimization algorithms but also to ensure low-cost evaluations and compliance with business intuitions.

We solve this bottleneck by capturing the DL surface with a lower-dimensional representation. We begin by leveraging the Adaptive Sparse Grids (ASG) algorithm [14, 23, 24, 44, 50] to translate the DL surface to a computationally cheap grid-based representation. Typically, grid-based representations suffer from a curse of dimensionality as the number of grid nodes increases exponentially with dimensionality (in this case, the number of marketplace levers we are optimizing). ASG solves this issue by limiting grid nodes to

locations that result in the highest contributions to accuracy and it serves as the foundation of the smoothing layer.

We then select B-spline functions as our smoothing model due to their flexibility and analytical derivative forms [22]. Unlike monotonic regression[36], B-splines offer the advantage of fitting derivatives, thereby avoiding optimization issues and aligning better with business intuition by providing continuous lever efficiencies rather than step-wise constants, B splines with quadratic basis functions allow us to enforce monotonicity and convexity, enhancing tractability [41], while Cox regression[48], often used in survival analysis, yields monotonically decreasing curves and is non-convex. Additionally, B-spline functions can adopt shape controls such as spot and universal derivative bounding, in a multidimensional treatment scenario, without parametric assumptions, thus reducing the risk of model misspecification. Furthermore, we enhance the model causal accuracy by integrating network effects-corrected budget efficiency experimental data through an additional penalty term in the objective function.

---

**Algorithm 1:** Adaptation algorithm: Build the grid iteratively

---

Begin with a starting grid;

**repeat**

    Compute hierarchical surplus at nodes; Find nodes with high hierarchical surplus, Add children nodes around these nodes

**Until** Recall hierarchical surplus measures residual error at each node, stop when all children nodes below maximum acceptable residual error  $|\epsilon_{add}|$ ;

---

**3.2.1 Adaptive Sparse Grid.** Adaptive sparse grids(ASG), constructed by preserving only a subset of the nodes on a dense grid, have been shown to maintain a comparable level of error while alleviating this curse of dimensionality [13, 42]. When the function representation is derived from linearly interpolating between nodes, errors in the representation stem from not having sufficient resolution in areas where the function is highly nonlinear. ASG iteratively refine the grid and add nodes where errors remain high. The adaptation process is governed by a score called the hierarchical surplus, which essentially measures how much the underlying objective function at a node deviates from a linear interpolation via the surrounding nodes. High values of the surplus imply uncaptured local curvature, and suggest additional nodes nearby could be useful. As an example, Figure 2 below shows how the adapted sparse grid places greater density around the nonlinear portion of the function  $f(x, y) = (|0.5 - x - y| + 0.1) - 1$ .

**3.2.2 B-Spline with Business Penalty.** We formulate each city’s cost surface smoothing as a constrained least square problem[12] in Equation (4). The fitting objective function consists of two parts. The first part is to minimize the sum of squared difference between B-spline smoothing model inferred  $obj_s(\mathbf{x}^g)$  and DL model inferred  $obj_r(\mathbf{x}^g)$  over all budget points  $\mathbf{x}^g = \{x_l | l = 1, \dots, N\}$  in search space grid  $G$ ; while the second part is to minimize the sum of squared difference between B-spline inferred budget efficiency and A/B experiment measured budget efficiency, which is essentially the

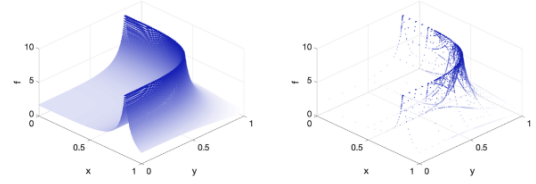


**Figure 2: Dense vs. Sparse Grid Representation**

$IOB$  introduced in Section 3.4. The variance of experimental data  $\sigma_l^2(\mathbf{x}^m)$  is incorporated as inverse weights to handle heteroscedasticity [45]. The hyperparameter  $\lambda$  determines the tradeoff between the objectives which can be tuned via cross-validation to optimize business impact defined in Equation 15.

$$\underset{obj_s(\cdot)}{\text{minimize}} \quad \sum_{\mathbf{x}^g \in G} (obj_s(\mathbf{x}^g) - obj_r(\mathbf{x}^g))^2 \quad (4)$$

$$+ \lambda \sum_{\mathbf{x}^m \in M} \sum_{l=1}^N \frac{1}{\sigma_l^2(\mathbf{x}^m)} (IOB_l(\mathbf{x}^m) - IOB_l(\mathbf{x}^m))^2$$

$$\text{s.t.} \quad obj_s(\mathbf{x}) = \sum_{i_1=0}^{n_1-1} \dots \sum_{i_N=0}^{n_N-1} a_{i_1 \dots i_N} \prod_{l=1}^N B_l^{r_l}(x_l; \mathbf{t}_l) \quad (5)$$

$$IOB_l(\mathbf{x}) = \frac{\partial obj_s(\mathbf{x})}{\partial x_l} \geq 0, \forall l \in \{1, \dots, N\} \quad (6)$$

$$\frac{\partial IOB_l(\mathbf{x})}{\partial x_l} \leq 0, \forall l \in \{1, \dots, N\} \quad (7)$$

where  $B_l^{r_l}(x_l; \mathbf{t}_l)$  is the  $i_l$ th B-Spline basis function of degree  $r_l$  over the knots  $\mathbf{t}_l$  for the  $l$ th incentive lever. The number of basis functions for  $l$ th lever is denoted as  $n_l$ . There are  $\prod_{l=1}^N n_l$  B-spline basis function coefficient  $a_{i_1 \dots i_N}$  to fit. Ignore the lever index  $l$  hereafter for simplicity. Knots  $\mathbf{t}$  consist of  $n - r + 1$  internal knots plus  $r$  boundary knots on each side. The complete knots vector  $\mathbf{t}$  is equal to  $\{t_0, \dots, t_{n+r}\}$ . Each basis function is defined by a recursive relationship. The 0th degree B-spline has the form

$$B_i^0(x; \mathbf{t}) = 1, \text{ if } t_i \leq x < t_{i+1}, \text{ otherwise } 0 \quad (8)$$

and higher degree B-splines are constructed as

$$B_i^r(x; \mathbf{t}) = \frac{x - t_i}{t_{i+r} - t_i} B_i^{r-1}(x; \mathbf{t}) + \frac{t_{i+r+1} - x}{t_{i+r+1} - t_{i+1}} B_{i+1}^{r-1}(x; \mathbf{t}) \quad (9)$$

The sufficient conditions of the non-negative return of  $l$ th lever over  $[t_{l,r_l}, t_{l,n_r}]$  can be shown as

$$a_{i_1 \dots i_l \dots i_N} - a_{i_1 \dots i_l - 1 \dots i_N} \geq 0, \forall i_l \quad (10)$$

and the sufficient conditions of the diminishing marginal return of  $l$ th lever can be shown as

$$\frac{a_{i_1 \dots i_l \dots i_N} - a_{i_1 \dots i_l - 1 \dots i_N}}{\Delta_{i_l}} \leq \frac{a_{i_1 \dots i_l - 1 \dots i_N} - a_{i_1 \dots i_l - 2 \dots i_N}}{\Delta_{i_l - 1}}, \forall i_l \quad (11)$$

where  $\Delta_{i_l} = t_{l, i_l + r_l} - t_{l, i_l}$ .

For a univariate B-spline with degree  $r = 2$ , the above conditions are also necessary. See Appendix C for details. Equations (10) and (11) are used to replace eqs. (6) and (7) to make the optimization problem tractable.

### 3.3 Optimizer

We use an optimization system to solve a global problem as described in Equation 1, which seeks to solve an objective maximization problem under constraints. While, as discussed in Sec. 3.2, we are able to guarantee monotonicity and concavity in individual dimensions, that does not extend to the entire surface.

In addition to the predictions from the *obj* estimator, we also introduce a penalty term in the form of Hellinger distance [28] that forces the system to prefer allocations similar to a reference allocation:

$$\text{pen}(\mathbf{b}_w, \mathbf{b}_0) = -\sqrt[3]{\max\left(\frac{\|\mathbf{b}_w\|}{\|\mathbf{b}_0\|}, \frac{\|\mathbf{b}_0\|}{\|\mathbf{b}_w\|}\right)} \times \sum_{c \in \text{cities}} \alpha_c \sum_{l \in \text{levers}} \kappa_l \sqrt{\frac{|b_{w,c,l}|}{\|\mathbf{b}_w\|} - \sqrt{\frac{|b_{0,c,l}|}{\|\mathbf{b}_0\|}}|^2}, \quad (12)$$

where  $\mathbf{b}_w$  is the budget vector for the week to be optimized,  $\mathbf{b}_0$  is the reference budget vector,  $\alpha_c$  and  $\kappa_l$  are scaling terms per city and lever, respectively, and the cube root term reduces the penalty term size as the budget difference increases, with the logic that the reference allocation should not be preferred if the total difference between the allocations is large.

In order to solve the non-linear, non-convex problem, which we know remains differentiable, we adopt an Alternating Direction Method of Multipliers (ADMM) [47] approach. Specifically, we separated the single-city cross-lever problem and the cross-city problem, and solved the problems iteratively.

Here is the reformation of the problem:

$$\begin{aligned} & \text{Minimize} \quad \sum_{c \in \text{cities}} f_c(\mathbf{b}_c) + g(\mathbf{z}) \\ & \text{subject to} \quad \mathbf{b}_c - \mathbf{z}_c = 0, c \in \text{cities} \end{aligned} \quad (13)$$

The resulting ADMM algorithm is,

$$\begin{aligned} \mathbf{b}_c^{k+1} & := \underset{\mathbf{b}_c}{\text{argmin}}(f_c(\mathbf{b}_c) + \rho/2 \|\mathbf{b}_c - \mathbf{z}^k + \mathbf{y}_c^k\|_2^2) \\ \mathbf{z}^{k+1} & := \underset{\mathbf{z}}{\text{argmin}}(g(\mathbf{z}) + \rho/2 \sum_{c \in \text{cities}} \|\mathbf{b}_c^{k+1} - \mathbf{z}_c + \mathbf{y}_c^k\|_2^2) \\ \mathbf{y}_c^{k+1} & := \mathbf{y}_c^k + \mathbf{b}_c^{k+1} - \mathbf{z}_c^{k+1}, \end{aligned} \quad (14)$$

where we slightly abuse the notation, as  $\mathbf{z}$  is the concatenation of  $\mathbf{z}_c \forall c \in \text{cities}$ . From the equations, we can summarize the algorithm in 3 steps:

- Update  $\mathbf{b}$  step, this step considers all the single city constraints.
- Update  $\mathbf{z}$  step, this step brings all the city together and only considers cross city optimization.
- Update  $\mathbf{y}$  step, this step updates the center of the update  $\mathbf{x}$  step.

Because our problem is close to convex, and the constraints applied to our smoothing model, by tuning  $\rho$ , we are able to ensure that the overall problem has a positive, semidefinite Hessian. The implementation of the algorithm is detailed in Appendix D.

### 3.4 Business Value Evaluation

In contrast to many other machine learning applications, which are mainly evaluated on predictive accuracy, our business use case requires us to predict marketplace outcomes for the coming weeks and generate budget allocations that maximize those outcomes. Therefore, we need a customized evaluation framework to measure

the quality of these budget allocations. One common approach, running large-scale experiments in the marketplace, is prohibitively costly and impractical for continuous model evaluation. Instead, we rely on existing A/B experiments that adjust budgets at the user level to estimate our business impact.

The Business Value Evaluation (BVE) framework combines existing A/B experimental data with simulated allocations to produce estimates that can be directly interpreted as weekly business impact. In particular, this can be calculated as:

$$\text{Business Impact} = \sum_{l,c} \int_{B_{l,c,old}}^{B_{l,c,new}} IOB_{l,c} dB \quad (15)$$

Where  $l$  indexes incentive levers and  $c$  denotes cities, and IOB is the implied return on additional budget from the existing A/B experimental data. To compute the integral, we take two approaches. (1) A linear approximation of the integral which implies simply computing the difference in budget between the optimal and actual allocations, then multiplying these differences by the return on this incremental budget. (2) A log-linear relationship between budgets and IOB and estimates this relationship from historical data. This ensures that we capture the curvature in the relationship between budget and IOB.

The key input of BVE is the incremental return on budget (IOB) which is estimated from user level A/B experiments which either make treatment more generous or target additional units. Given these continuously running experiments, we can measure the lift of an additional dollar budget on our *obj* with the following regression as:

$$obj_i = \alpha + \beta \times Treatment_i + X_i \theta + \epsilon_i$$

Where  $i$  refers to a treated unit and  $X_i$  are a vector of pre-XP covariates. Adding in controls into this regression framework allows us to soak up idiosyncratic noise and increase precision [6]. The coefficient gives us the incremental lift on *obj* per user (iO). Moreover, for each of these XPs, the incremental budget per user (iB) is deterministic and given by the XP design. This implies that we can compute  $\frac{\Delta obj}{\Delta B}$ .

The main challenge in computing IOB based on unit level A/Bs at Uber is the presence of network effects or spillover effects. What makes this a unique problem without standard off the shelf solutions is that the Uber marketplace has multiple rationing mechanisms during periods of relative undersupply; namely prices and ETAs (expected time to arrival). This implies that the Stable Unit Treatment Value Assumption (SUTVA) is often violated, where outcomes for one unit depends on the treatment assignments of others. As a simple example, allocating budget towards incentives which boost demand when there is acute undersupply can lead to user level A/B effects grossly overestimating the true marketplace effect. The key mechanism behind this is that treated users on the demand side of the market might cannibalize supply which would have been otherwise available to the control group users. To account for this issue, we developed an economic model which predicts the incremental marketplace changes in endogenous quantities such as our *obj* to changes in exogenous quantities like supply and demand. This model is characterized by a set of key elasticities which govern how both users and aggregate marketplace outcomes respond to changes in Uber's rationing mechanisms; prices and ETAs.

The paper closest in spirit to our approach is [16] which develops a marketplace model to understand how pricing can prevent the market from reaching undesirable equilibria. Our approach is also similar to recent papers in the literature [3, 9, 15] which develop marketplace models in ride-sharing markets to study optimal pricing and matching policies. With key elasticities estimated from previously run XPs, we can predict the change in our *obj* due to changes in model inputs such sessions and supply hours. We then use a first-order Taylor approximation to translate A/B outcomes into marketplace outcomes in the following way:

$$\text{Marketplace Effect on Obj} = (\text{Effect of Model Inputs on Obj}) \times (\text{A/B Effect on Model Inputs})$$

Taking driver promotions as example, this implies that we use the calibrated model’s implied effect on marketplace outcomes such as our *obj* due to changes in supply and the A/B effect on supply to compute the marketplace effect on *obj*.

## 4 EVALUATION AND RESULTS

We conducted comprehensive backtesting using Uber marketplace historical data to evaluate the efficacy and robustness of our proposed methodology. This approach allows us to measure incremental out-of-sample performance and the business impact of counterfactual budget allocations from our system, all while fully accounting for complexities in the underlying data generating process

We begin with predictive accuracy to ensure our model captures marketplace dynamics effectively. We compute wMAPE (weighted Mean Absolute Percentage Error) and wBIAS (weighted BIAS) at the city-week level, appropriately weighting cities of varying sizes and matches the granularity of the budget allocation decision. Table 1 shows how these metrics vary across methodologies and regions. Across both regions, the Causal DL model substantially outperforms the stacked Estimator model in terms of wMAPE and wBIAS.

We complement these predictive accuracy metrics with business impact metrics from the aforementioned Business Value Evaluation framework in Section 3.4. Internally, we compute business impact from Equation 15 in terms of *obj* when comparing candidate models for production usage. While we are unable to share this directly, we can share the following closely related metric for each model:

$$\text{Marginal Efficiency} = \frac{\sum_{l,c} B_{l,c,opt} \times IOB_{l,c}}{\sum_{l,c} B_{l,c,opt}}$$

Marginal efficiency captures the value of an additional dollar of budget allocated proportionally to all cities and levers by weighting efficiency estimates accordingly. High marginal efficiency implies budgets are being deployed in an efficient manner. Table 2 reports the percentage change in this metric against a baseline model for our backtests which show that the Causal DL model with model enhancements outperforms the baseline model in both regions.

Finally, Figure 3 shows an example of how budget allocations differ across select cities (y-axis) and weeks (x-axis) between two different models. Colors and annotations indicate the percentage change in budgets across the models. Importantly, note how the budget differences are mostly small. This allows us to comfortably use a linearized version of Equation 15 to measure business impact.

**Table 1: Prediction accuracy between stacked Estimator and Causal ML model**

Dataset		Region US	Region BR
Method	Metric		
LGBM baseline	wMAPE %	7.109	7.454
	wBIAS %	-0.687	-1.863
Causal DL	wMAPE %	<b>3.264</b>	<b>5.622</b>
	wBIAS %	<b>-0.115</b>	<b>0.645</b>

**Table 2: Marginal efficiency by method and region, percentage improvements relative to baseline model**

Method	Region US	Region BR
Causal DL w/ business penalty	9.23%	2.59%
Causal DL w/ endogeneity fix	8.00%	0.82%

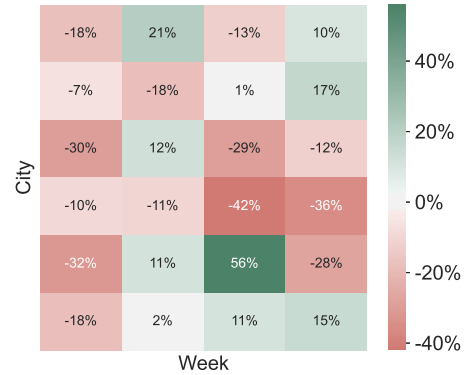


**Figure 3: Budget differences between two models**

## 5 CONCLUSION

We present an end-to-end causal machine learning and optimization system designed to enhance Uber’s marketplace budget allocation process. This system automates weekly budgeting decisions to maximize marketplace objectives within predefined constraints, improving overall operational efficiency. Our approach addresses a high-dimensional optimization problem involving various marketplace levers and their respective budgets. To solve this, we employ a deep learning estimator based on an S-Learner approach, leveraging extensive experimental and temporal-spatial observational data to estimate causal effects. We also incorporate a tensor B-Spline regression model that captures the detailed response surface of DL models while ensuring practical efficiency. Additionally, our system utilizes ADMM and primal-dual interior point convex optimization techniques, implemented on Ray, to handle large-scale nonlinear, non-convex problems efficiently. The deployment of this system not only simplifies decision-making but ensures these decisions are data-driven and aligned with Uber’s strategic objectives.

## ACKNOWLEDGMENTS

This work was supported by Uber Technologies Inc.

## REFERENCES

- [1] Uber announces results for third quarter 2023, 11 2023.
- [2] Amir Ali Ahmadi, Alex Olshevsky, Pablo A Parrilo, and John N Tsitsiklis. N-hardness of deciding convexity of quartic polynomials and related problems. *Mathematical Programming*, 137:453–476, 2013.
- [3] Motaz Al-Chanati and Vinayak Iyer. What drives the efficiency in ridesharing markets? evidence from austin, texas. Available at SSRN 3959363, 2021.
- [4] Martin Andersen, Joachim Dahl, and Lieven Vandenbergh. Cvxopt: Convex optimization. *Astrophysics Source Code Library*, pages ascl–2008, 2020.
- [5] Adebisi A Ariyo, Adewumi O Adewumi, and Charles K Ayo. Stock price prediction using the arima model. In *2014 UKSim-AMSS 16th international conference on computer modelling and simulation*, pages 106–112. IEEE, 2014.
- [6] Susan Athey and Guido Imbens. The econometrics of randomized experiments, 2016.
- [7] Susan Athey and Guido Imbens. Recursive partitioning for heterogeneous causal effects. *Proceedings of the National Academy of Sciences*, 113(27):7353–7360, 2016.
- [8] Domenico Benvenuto, Marta Giovanetti, Lazzaro Vassallo, Silvia Angeletti, and Massimo Ciccozzi. Application of the arima model on the covid-2019 epidemic dataset. *Data in brief*, 29:105340, 2020.
- [9] Kostas Bimpikis, Ozan Candogan, and Daniela Saban. Spatial pricing in ride-sharing networks. *Operations Research*, 67(3):744–769, 2019.
- [10] Grigoriy Blekherman, Pablo A Parrilo, and Rekha R Thomas. *Semidefinite optimization and convex algebraic geometry*. SIAM, 2012.
- [11] George Edward Pelham Box and Gwilym Jenkins. *Time Series Analysis, Forecasting and Control*. Holden-Day, Inc., USA, 1990.
- [12] Stephen Boyd and Lieven Vandenbergh. *Introduction to applied linear algebra: vectors, matrices, and least squares*. Cambridge university press, 2018.
- [13] Johannes Brumm and Simon Scheidegger. Using adaptive sparse grids to solve high-dimensional dynamic models. *Econometrica*, 85(5):1575–1612, 2017.
- [14] Hans-Joachim Bungartz and Michael Griebel. Sparse grids. *Acta Numerica*, 13:1–123, 2004.
- [15] Juan Camilo Castillo. Who benefits from surge pricing? Available at SSRN 3245533, 2023.
- [16] Juan Camilo Castillo, Dan Knoepfle, and Glen Weyl. Surge pricing solves the wild goose chase. In *Proceedings of the 2017 ACM Conference on Economics and Computation*, pages 241–242, 2017.
- [17] Si-An Chen, Chun-Liang Li, Nate Yoder, Sercan O Arik, and Tomas Pfister. Tsmixer: An all-mlp architecture for time series forecasting. *arXiv preprint arXiv:2303.06053*, 2023.
- [18] Victor Chernozhukov, Denis Chetverikov, Mert Demirer, Esther Duflo, Christian Hansen, Whitney Newey, and James Robins. Double/debiased machine learning for treatment and structural parameters, 2018.
- [19] Carl De Boor. On calculating with b-splines. *Journal of Approximation theory*, 6(1):50–62, 1972.
- [20] Carl De Boor and Carl De Boor. *A practical guide to splines*, volume 27. Springer-Verlag New York, 1978.
- [21] Shuyang Du, James Lee, and Farzin Ghaffarizadeh. Improve user retention with causal learning. In *The 2019 ACM SIGKDD Workshop on Causal Discovery*, pages 34–49. PMLR, 2019.
- [22] Paul HC Eilers and Brian D Marx. Flexible smoothing with b-splines and penalties. *Statistical science*, 11(2):89–121, 1996.
- [23] Michael Griebel. A parallelizable and vectorizable multi-level algorithm on sparse grids. In *Parallel algorithms for partial differential equations*, 1991.
- [24] Michael Griebel, Michael Schneider, and Christoph Zenger. A combination technique for the solution of sparse grid problems. In *Iterative Methods in Linear Algebra*, page 263–281, 1992.
- [25] P Richard Hahn, Jared S Murray, and Carlos M Carvalho. Bayesian regression tree models for causal inference: Regularization, confounding, and heterogeneous effects (with discussion). *Bayesian Analysis*, 15(3):965–1056, 2020.
- [26] Simon Haykin. *Neural networks: a comprehensive foundation*. Prentice Hall PTR, 1994.
- [27] Kaiming He, Xiangyu Zhang, Shaoqing Ren, and Jian Sun. Deep residual learning for image recognition, 2015.
- [28] Ernst Hellinger. Neue begründung der theorie quadratischer formen von unendlichvielen veränderlichen. *Journal für die reine und angewandte Mathematik*, 1909(136):210–271, 1909.
- [29] Aaron D. Hill, Scott G. Johnson, Lindsey M. Greco, Ernest H. O’Boyle, and Sheryl L. Walter. Endogeneity: A review and agenda for the methodology-practice divide affecting micro and macro research. *Journal of Management*, 47(1):105–143, 2021.
- [30] Jennifer L Hill. Bayesian nonparametric modeling for causal inference. *Journal of Computational and Graphical Statistics*, 20(1):217–240, 2011.
- [31] Yuchen Hu, Shuangning Li, and Stefan Wager. Average direct and indirect causal effects under interference. *Biometrika*, 109(4):1165–1172, 2022.
- [32] Kosuke Imai and Marc Ratkovic. Estimating treatment effect heterogeneity in randomized program evaluation. 2013.
- [33] Sören R Künzel, Jasjeet S Sekhon, Peter J Bickel, and Bin Yu. Metalearners for estimating heterogeneous treatment effects using machine learning. *Proceedings of the national academy of sciences*, 116(10):4156–4165, 2019.
- [34] Shiyang Li, Xiaoyong Jin, Yao Xuan, Xiyu Zhou, Wenhui Chen, Yu-Xiang Wang, and Xifeng Yan. Enhancing the locality and breaking the memory bottleneck of transformer on time series forecasting. *Advances in neural information processing systems*, 32, 2019.
- [35] Bryan Lim, Sercan Ö Arik, Nicolas Loeff, and Tomas Pfister. Temporal fusion transformers for interpretable multi-horizon time series forecasting. *International Journal of Forecasting*, 37(4):1748–1764, 2021.
- [36] Ziqi Liu, Dong Wang, Qianyu Yu, Zhiqiang Zhang, Yue Shen, Jian Ma, Wenliang Zhong, Jinjie Gu, Jun Zhou, Shuang Yang, and Yuan Qi. Graph representation learning for merchant incentive optimization in mobile payment marketing. In *Proceedings of the 28th ACM International Conference on Information and Knowledge Management*, CIKM ’19, page 2577–2584, New York, NY, USA, 2019. Association for Computing Machinery.
- [37] Philipp Moritz, Robert Nishihara, Stephanie Wang, Alexey Tumanov, Richard Liaw, Eric Liang, Melih Elibol, Zongheng Yang, William Paul, Michael I Jordan, et al. Ray: A distributed framework for emerging {AI} applications. In *13th USENIX symposium on operating systems design and implementation (OSDI 18)*, pages 561–577, 2018.
- [38] Yu E Nesterov and Michael J Todd. Primal-dual interior-point methods for self-scaled cones. *SIAM Journal on optimization*, 8(2):324–364, 1998.
- [39] Xinkun Nie and Stefan Wager. Quasi-oracle estimation of heterogeneous treatment effects. *Biometrika*, 108(2):299–319, 2021.
- [40] Scott Powers, Junyang Qian, Kenneth Jung, Alejandro Schuler, Nigam H Shah, Trevor Hastie, and Robert Tibshirani. Some methods for heterogeneous treatment effect estimation in high dimensions. *Statistics in medicine*, 37(11):1767–1787, 2018.
- [41] Natalya Pya and Simon N Wood. Shape constrained additive models. *Statistics and computing*, 25:543–559, 2015.
- [42] Andreas Schaab and Allen T Zhang. Dynamic programming in continuous time with adaptive sparse grids. *Working Paper*, 2022.
- [43] Uri Shalit, Fredrik D Johansson, and David Sontag. Estimating individual treatment effect: generalization bounds and algorithms. In *International conference on machine learning*, pages 3076–3085. PMLR, 2017.
- [44] Sergei Abramovich Smolyak. Quadrature and interpolation formulas for tensor products of certain classes of functions. *Doklady Akademii Nauk*, 148:1042–1045, 1963.
- [45] Tilo Strutz. *Data fitting and uncertainty: A practical introduction to weighted least squares and beyond*, volume 1. Springer, 2011.
- [46] Ashish Vaswani, Noam Shazeer, Niki Parmar, Jakob Uszkoreit, Llion Jones, Aidan N. Gomez, Lukasz Kaiser, and Illia Polosukhin. Attention is all you need. *CoRR*, abs/1706.03762, 2017.
- [47] Yu Wang, Wotao Yin, and Jinshan Zeng. Global convergence of admm in non-convex nonsmooth optimization. *Journal of Scientific Computing*, 78:29–63, 2019.
- [48] Li Yu, Zhengwei Wu, Tianchi Cai, Ziqi Liu, Zhiqiang Zhang, Lihong Gu, Xiaodong Zeng, and Jinjie Gu. Joint incentive optimization of customer and merchant in mobile payment marketing. *Proceedings of the AAAI Conference on Artificial Intelligence*, 35(17):15000–15007, May 2021.
- [49] Ailing Zeng, Muxi Chen, Lei Zhang, and Qiang Xu. Are transformers effective for time series forecasting? In *Proceedings of the AAAI conference on artificial intelligence*, volume 37, pages 11121–11128, 2023.
- [50] Christoph Zenger. Sparse grids. In *Proceedings of the Research Workshop of the Israel Science Foundation on Multiscale Phenomenon, Modelling and Computation*, page 86, 1991.
- [51] Haoyi Zhou, Shanghang Zhang, Jieqi Peng, Shuai Zhang, Jianxin Li, Hui Xiong, and Wancai Zhang. Informer: Beyond efficient transformer for long sequence time-series forecasting. In *Proceedings of the AAAI conference on artificial intelligence*, volume 35, pages 11106–11115, 2021.
- [52] Tian Zhou, Ziqing Ma, Qingsong Wen, Liang Sun, Tao Yao, Wotao Yin, Rong Jin, et al. Film: Frequency improved legendre memory model for long-term time series forecasting. *Advances in Neural Information Processing Systems*, 35:12677–12690, 2022.
- [53] Tian Zhou, Ziqing Ma, Qingsong Wen, Xue Wang, Liang Sun, and Rong Jin. Fedformer: Frequency enhanced decomposed transformer for long-term series forecasting. In *International Conference on Machine Learning*, pages 27268–27286. PMLR, 2022.

## A SYSTEM OVERVIEW

An end-to-end view containing all components of the budget allocation system described in this paper can be found in Fig. 4.

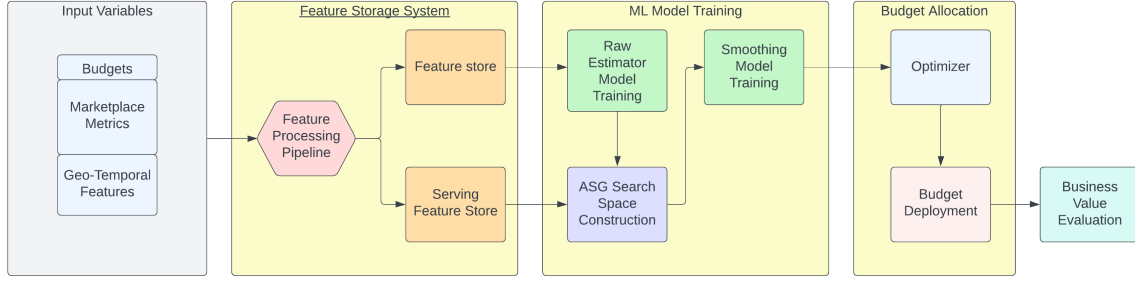


Figure 4: Allocation system architecture: raw data processing into feature store, ML model training and serving, optimization, and evaluation.

## B METALEARNER COMPARISON

In Table 3, we evaluate the predicted incremental supply efficiency of the S-learner with percentage error (BIAS) at the city-week granularity, which shows closer alignment with experimental ground truth compared to the R-learner. The untuned S-learner model exhibits a median BIAS similar to the current baseline performance. Unlike the baseline, the S-learner does not consistently underestimate lever efficiency, though certain weeks display significant prediction errors.

## C B-SPLINE PROOFS

In this section, we discuss the monotonicity and concavity conditions of B-spline functions in more details and provide some proofs.

PROPOSITION C.1. *Given a univariate B-spline function*

$$S(x) = \sum_{i=0}^{n-1} a_i B_i^r(x; t) \quad (16)$$

with knots  $t = \{t_0, \dots, t_{n+1}\}$ , the sufficient condition for  $S(x)$  to be monotonically non-decreasing over  $[t_r, t_n]$  is

$$a_i - a_{i-1} \geq 0, \quad i = 1, \dots, n-1 \quad (17)$$

PROOF. Following [19, 20], the first order derivative of  $S(x)$  with respect to  $x$  can be written as

$$\frac{\partial S(x)}{\partial x} = \sum_{i=1}^{n-1} \frac{r}{\Delta_i} (a_i - a_{i-1}) B_i^{r-1}(x; t') \quad (18)$$

where  $\Delta_i = t_{i+r} - t_i$ .

Note that  $\frac{\partial S(x)}{\partial x}$  is a new B-spline function with degree  $r-1$  and knots  $t' = t[1: -1]$ . Since by definition (Equations (8) and (9)), B-spline basis  $B_i^{r-1}(x; t')$  cannot be negative. Given  $\Delta_i \geq 0$ , it is clear that if  $a_i - a_{i-1} \geq 0$  for  $i = 1, \dots, n-1$ , then  $\frac{\partial S(x)}{\partial x} \geq 0$   $\square$

PROPOSITION C.2. *Given a univariate B-spline function*

$$S(x) = \sum_{i=0}^{n-1} a_i B_i^r(x; t) \quad (19)$$

with knots  $t = \{t_0, \dots, t_{n+1}\}$ , the sufficient condition for  $S(x)$  to be concave over  $[t_r, t_n]$  is

$$\frac{a_i - a_{i-1}}{\Delta_i} - \frac{a_{i-1} - a_{i-2}}{\Delta_{i-1}} \leq 0, \quad i = 2, \dots, n-1 \quad (20)$$

where  $\Delta_i = t_{i+r} - t_i$

PROOF. Based on Equation (18), the second order derivative of  $S(x)$  with respect to  $x$  can be written as

$$\begin{aligned} \frac{\partial^2 S(x)}{\partial x^2} &= \sum_{i=2}^{n-1} \frac{r-1}{t_{i+r-1} - t_i} \left[ \frac{r}{\Delta_i} (a_i - a_{i-1}) \right. \\ &\quad \left. - \frac{r}{\Delta_{i-1}} (a_{i-1} - a_{i-2}) \right] B_i^{r-2}(x; t'') \end{aligned} \quad (21)$$

where  $\Delta_i = t_{i+r} - t_i$ .

Note that  $\frac{\partial^2 S(x)}{\partial x^2}$  is a new B-spline function with degree  $r-2$  and knots  $t'' = t[2: -2]$ .

Similarly, since B-spline basis  $B_i^{r-2}(x; t'')$  and  $t_{i+r-1} - t_i$  are non-negative, it is clear that if  $\frac{r}{\Delta_i} (a_i - a_{i-1}) - \frac{r}{\Delta_{i-1}} (a_{i-1} - a_{i-2}) \leq 0$  for  $i = 2, \dots, n-1$ , then  $\frac{\partial^2 S(x)}{\partial x^2} \leq 0$   $\square$

PROPOSITION C.3. *Given a univariate B-spline function*

$$S(x) = \sum_{i=0}^{n-1} a_i B_i^r(x; t) \quad (22)$$

with knots  $t = \{t_0, \dots, t_{n+1}\}$ , when the basis function degree  $r = 2$ , Equation (17) is also a necessary condition for  $S(x)$  to be monotonically non-decreasing over  $[t_2, t_n]$

PROOF. When  $r = 2$ , the first order derivative in Equation (18) can be written as

$$\frac{\partial S(x)}{\partial x} = \sum_{i=1}^{n-1} \frac{2}{\Delta_i} (a_i - a_{i-1}) B_i^1(x; t') \quad (23)$$

where  $\Delta_i = t_{i+2} - t_i$ .

By Lemma C.4, when  $x \in [t_i, t_{i+1})$ ,  $\frac{\partial S(x)}{\partial x}$  can be written as

$$\frac{\partial S(x)}{\partial x} = \frac{2}{\Delta_i} (a_i - a_{i-1}) \frac{x - t_i}{t_{i+1} - t_i} \quad (24)$$

It is clear that  $\frac{\partial S(x)}{\partial x} \geq 0$  only if  $a_i - a_{i-1} \geq 0$ . It is straightforward to generalize this for all  $x \in [t_2, t_n]$   $\square$

LEMMA C.4. *The degree 1 B-spline basis function  $B_i^1(x; t) = \frac{x - t_i}{t_{i+1} - t_i}$  for  $x \in [t_i, t_{i+1})$*



**Table 3: Comparison of S-Learner and R-Learner Incremental Supply Efficiency Predictions**

Week	Experiment	Baseline Prediction	S-Learner Prediction	S-Learner BIAS	R-Learner Prediction	R-Learner BIAS
week 1	0.029	0.012	0.087	0.058	0.193	0.501
week 2	0.045	0.010	0.017	-0.029	0.314	0.125
week 3	0.053	0.010	0.349	0.295	0.113	0.720
week 4	0.045	0.008	0.621	0.576	0.314	0.478
week 5	0.027	0.009	0.104	0.077	0.368	0.132
week 6	0.045	0.008	0.026	-0.019	0.385	0.086
week 7	0.053	0.013	0.075	0.022	0.660	0.387
week 8	0.046	0.016	0.015	-0.030	0.182	0.614

PROOF. Based on Equation (8), when  $x \notin [t_i, t_{i+1})$ , we have  $B_i^0(x; \mathbf{t}) = 0$

Then, based on Equation (9), we have

$$B_i^1(x; \mathbf{t}) = \begin{cases} \frac{x-t_i}{t_{i+1}-t_i} & \text{when } x \in [t_i, t_{i+1}) \\ 0 & \text{otherwise} \end{cases} \quad (25)$$

□

PROPOSITION C.5. *Given a univariate B-spline function*

$$S(x) = \sum_{i=0}^{n-1} a_i B_i^r(x; \mathbf{t}) \quad (26)$$

with knots  $\mathbf{t} = \{t_0, \dots, t_{n+1}\}$ , when the basis function degree  $r = 2$ , Equation (20) is also a necessary condition for  $S(x)$  to be concave over  $[t_2, t_n]$

PROOF. When  $r = 2$ , the second order derivative in Equation (21) can be written as

$$\frac{\partial^2 S(x)}{\partial x^2} = \sum_{i=2}^{n-1} \frac{1}{t_{i+1} - t_i} \left[ \frac{2}{\Delta_i} (a_i - a_{i-1}) \right. \quad (27)$$

$$\left. - \frac{2}{\Delta_{i-1}} (a_{i-1} - a_{i-2}) \right] B_i^0(x; \mathbf{t}'') \quad (28)$$

where  $\Delta_i = t_{i+2} - t_i$  and knots  $\mathbf{t}'' = \mathbf{t}[2: -2]$ .

Based on Equation (8), for any  $t_{2+i} \leq x < t_{2+i+1}$ ,  $i = 0, \dots, n-1$ ,  $\frac{\partial^2 S(x)}{\partial x^2}$  is equal to

$$\frac{\partial^2 S(x)}{\partial x^2} = \frac{2}{\Delta_i} (a_i - a_{i-1}) - \frac{2}{\Delta_{i-1}} (a_{i-1} - a_{i-2}) \quad (29)$$

because other bases are 0.

It is clear that  $\frac{\partial^2 S(x)}{\partial x^2} \leq 0$  over  $[t_2, t_n]$  only if  $\frac{2}{\Delta_i} (a_i - a_{i-1}) - \frac{2}{\Delta_{i-1}} (a_{i-1} - a_{i-2}) \leq 0, \forall i$

□

PROPOSITION C.6. *Propositions C.1 and C.2 can be generalized to any multivariate B-spline function.*

PROOF. A multivariate B-spline function can be written as

$$S(x_1, \dots, x_N) = \sum_{i_1=0}^{n_1-1} \dots \sum_{i_N=0}^{n_N-1} a_{i_1 \dots i_N} \prod_{l=1}^N B_{i_l}^{r_l}(x_l; \mathbf{t}_l) \quad (30)$$

Without loss of generality, assume we are interested in its partial derivative with respect to  $x_j$ .  $S(x_1, \dots, x_N)$  can be re-arranged as follows to separate items involving  $x_j$  and others

$$S(x_1, \dots, x_N) = \sum_{i_1=0}^{n_1-1} \dots \sum_{i_N=0}^{n_N-1} \prod_{l=1, l \neq j}^N B_{i_l}^{r_l}(x_l; \mathbf{t}_l) \sum_{i_j=0}^{n_j-1} a_{i_1 \dots i_N} B_{i_j}^{r_j}(x_j; \mathbf{t}_j) \quad (31)$$

Denote

$$C(x_{l \neq j} | i_{l \neq j}) = \prod_{l=1, l \neq j}^N B_{i_l}^{r_l}(x_l; \mathbf{t}_l) \quad (32)$$

it is always non-negative because it is a product of multiple B-spline bases and each B-spline basis cannot be negative by definition.

Denote

$$S(x_j | i_{l \neq j}) = \sum_{i_j=0}^{n_j-1} a_{i_1 \dots i_N} B_{i_j}^{r_j}(x_j; \mathbf{t}_j) \quad (33)$$

it is a univariate B-spline function.

$S(x_1, \dots, x_N)$  can be written as

$$S(x_1, \dots, x_N) = \sum_{i_1=0}^{n_1-1} \dots \sum_{i_N=0}^{n_N-1} C(x_{l \neq j} | i_{l \neq j}) S(x_j | i_{l \neq j}) \quad (34)$$

The derivative of  $S(x_1, \dots, x_N)$  with respect to  $x_j$  is equal to a sum of non-negative  $C(x_{l \neq j} | i_{l \neq j})$  times the derivative of univariate B-spline  $S(x_j | i_{l \neq j})$  with respect to  $x_j$ . Hence, Propositions C.1 and C.2 for a univariate B-spline function can be extended to a multivariate B-spline function. □

## D OPTIMIZER IMPLEMENTATION

In order to solve the per-city problems in the  $\mathbf{b}$ -update step, we use `cvxopt` [4], which is a primal-dual interior-point convex solver that uses Nesterov-Todd scaling [38]. Since the modified problem is both city-independent and convex, this inner solver works well for us.

A major challenge to solving the problem in a single thread, instead of in parallel, is that the constraint complexity is high, and collinear constraints can affect the Cholesky decomposition in the Nesterov-Todd scaling step. The single city constraints are much easier to manage and therefore never cause this problem in the `cvxopt` step. Regardless, managing constraints, including online validations when receiving constraints from client teams remains a key practical effort of the system.

Recall that our constraints that cross multiple cities are equality constraints. Therefore,  $g(z)$  in Equation 13 is essentially an indicator function that is zero-valued when the constraint is met and takes a large value when the constraint is not met.

The update  $z$  step can therefore be translated to a simple quadratic optimization problem. We can then use the Cauchy-Schwartz inequality to simplify further, eventually resulting in an algebraic expression, that for the constraint in Equation 1, results in:

$$\mathbf{z}_c^{k+1} := \frac{B - \mathbf{e} \cdot \sum_{c \in \text{cities}} \mathbf{u}_c^k}{|C||L|} \mathbf{e} + \mathbf{u}_c^k, \quad (35)$$

where  $\mathbf{u}_c^k := \mathbf{y}_c^k + \mathbf{b}_c^{k+1}$  and  $\mathbf{e}$  is a vector of all ones. This simplification allows the update  $z$  step to be calculated algebraically.

Several practical improvements allow the system to scale well and perform with high stability in production:

- **Horizontal scaling with Ray.** [37] Because the update  $x$  step is handling each city individually, we can run optimization for each city in parallel. By leveraging the Ray

framework, we achieved approximately a 50x speedup per iteration in that step.

- **Adaptive  $\rho$ .** In order to improve stability of the system, we adaptively increase  $\rho$  when non-convex sub-problems are detected. As mentioned above, this modifies the eigenvalues of the Hessian to ensure convexness.
- **Early Stopping & Optimal criteria.** The ADMM algorithm can quickly get to a point where it is close to the global optima, but it takes a long time to provide a solution with multi-digit accuracy. Our implementation requires a compromise between runtime and accuracy. We define a solution is optimal if:
  - Constraints are obeyed within 0.1% accuracy
  - All sub problems (single city) are converged
  - The change in objective value is small from the previous iteration
  - Primal and dual feasibility are satisfied